Supporting Information

Tait et al. 10.1073/pnas.1008242107

SI Text

Isothermal Titration Calorimetry and Circular Dichroism. For ITC, samples were dialyzed twice into filtered and degassed sample buffer (10 mM Tris pH 6.5, 50 mM KCl). eIF4E was concentrated using Sartorius Vivaspin 6-mL concentrators (10 kD M_r cutoff). Samples were clarified by centrifuging at full speed for 1 min in a benchtop centrifuge. ITC was performed on a VP-ITC machine (MicroCal) using 10 μM of purified eIF4E and 100–300 μM of peptide. CD measurements were performed using a Jasco J-810 spectropolarimeter.

NMR. All ^{15}N-^{13}C-labeled peptides were resuspended in 50 mM KCl, 10 mM Tris-d11, pH 6.5. Experiments were performed at 25 °C using 500- and 700-MHz Bruker spectrometers equipped with cryoprobes. Backbone assignments were done via ^{1}H-{^{15}N} HSQC, HNCO nuclei triple resonance experiment, HNCαCβ nuclei triple resonance experiment (HNCACB), and CβCαCONH nuclei triple resonance experiment (CBCACONH). $^{3}J_{\mathrm{NH\text{-}H}\alpha}$ coupling constants (3D-HNHA; ref. 1) were measured using eight transients, and calculated from cross-peak/diagonal peak ratios. Twenty-five micromolar [U-^{15}N,^{13}C] peptides (WT and phosWT) in 50 mM KCl, 10 mM [U-2H] Tris, pH 6.5 was used for recording the ^{1}H-^{15}N HSQC spectra of the complex with 25 μM of unlabeled eIF4E using 256 transients. The ^{1}H chemical shifts were referenced to water at 4.75 ppm (at 25 °C), and the ^{13}C and ^{15}N chemical shifts were referenced indirectly using the $\gamma^{13}\mathrm{C}/\gamma^{1}\mathrm{H}$ and $\gamma^{15}\mathrm{N}/\gamma^{1}\mathrm{H}$ ratios, respectively. All spectra were processed using nmrPipe, visualized with nmrDraw (2) and analyzed using NMRView (3). The chemical shift difference between the WT and mutants (M60E and R63Q), and phosphorylated WT were calculated using the equation $\sqrt{(\Delta\delta_{\mathrm{HN}})^2 + (0.25 * \Delta\delta_{\mathrm{N}})^2}$, where $\Delta\delta_{\mathrm{HN}}$ and $\Delta\delta_{\mathrm{N}}$ are the changes in the chemical shifts of ^{1}H and ^{15}N dimension, plotted against residue number.

Modeling Procedures. Swiss PDB Viewer (4) was used to add V67 for sequence visualization in the context of the available structure (PDB ID code 1wkw; ref. 5). Molecular graphics images were constructed using PyMOL (http://www.pymol.org). Calculations of charge interactions between a modeled phosphorylated S65 of 4E-BP1, and acidic groups in eIF4E, followed previously reported methodology (6). A charge of −2e was placed on the OG atom of serine, and electrostatic interactions were computed using Debye–Huckel and finite difference Poisson–Boltzmann methods.

1. Vuister G, Bax A (1993) Quantitative J correlation: A new approach for measuring homonuclear three-bond $J(H^{N}H^{a})$ coupling constants in ^{15}N enriched proteins. *J Am Chem Soc* 115:7772–7777.
2. Delaglio F, et al. (1995) NMRPipe: A multidimensional spectral processing system based on UNIX pipes. *J Biomol NMR* 6:277–293.
3. Johnson BA (2004) Using NMRView to visualize and analyze the NMR spectra of macromolecules. *Methods Mol Biol* 278:313–352.
4. Guex N, Peitsch MC (1997) SWISS-MODEL and the Swiss-PdbViewer: An environment for comparative protein modelling. *Electrophoresis* 18:2714–2723.
5. Tomoo K, et al. (2005) Structural basis for mRNA cap-binding regulation of eukaryotic initiation factor 4E by 4E-binding protein, studied by spectroscopic, X-ray crystal structural, and molecular dynamics simulation methods. *Biochim Biophys Acta* 1753:191–208.
6. Kitchen J, Saunders RE, Warwicker J (2008) Charge environments around phosphorylation sites in proteins *BMC Struct Biol* 8:19.

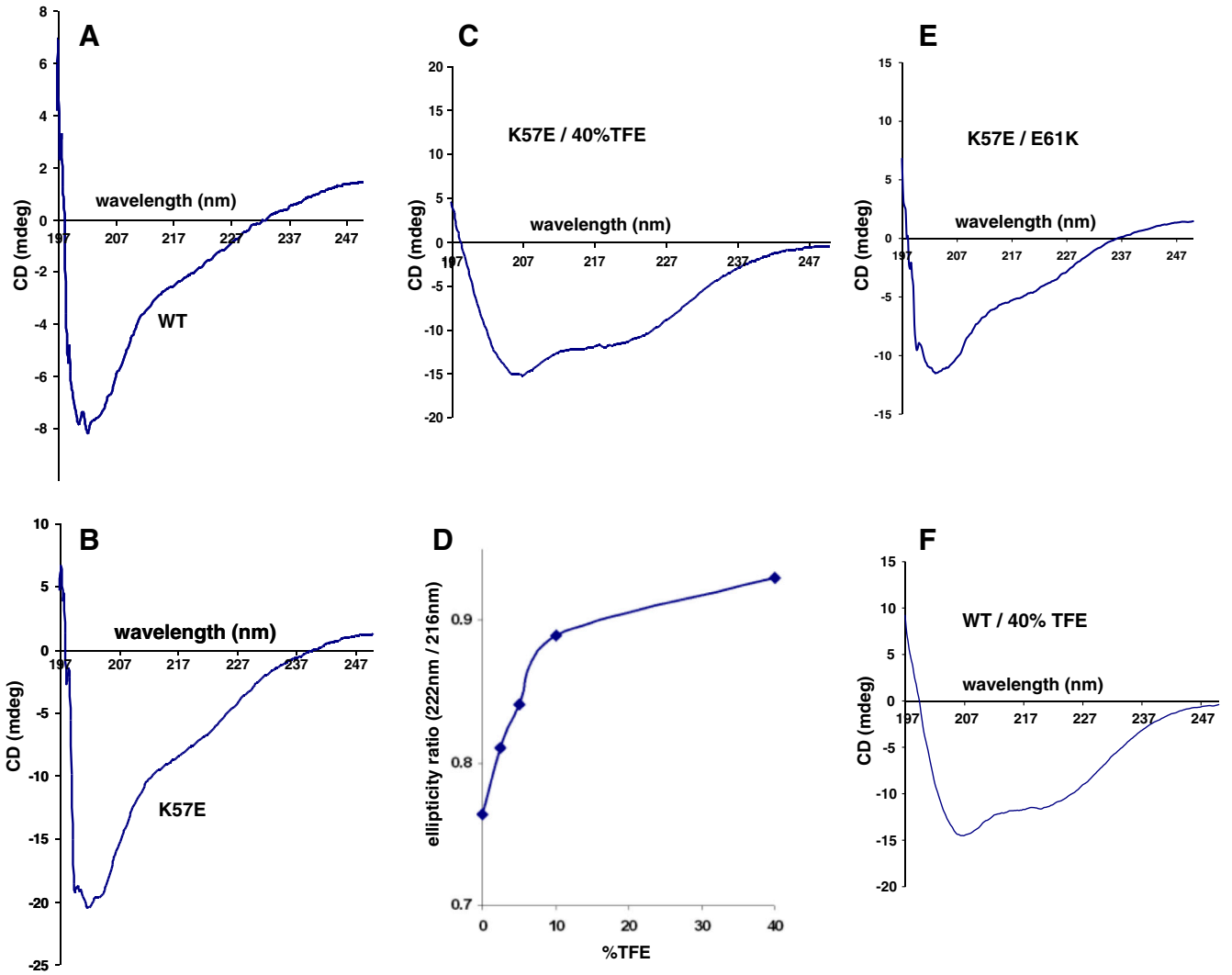

Fig. S1. Circular dichroism spectroscopy plots showing the dependence of ellipticity per residue as a function of wavelength in the far-UV spectral region for the 4E-BP1$_{51–67}$ peptides wild type (*A*) and K57E (*B*). The K57E spectrum changed significantly in the presence of 40% trifluoroethanol (TFE) (*C*); this was a progressive change with increasing TFE concentration, as shown by the plot of the ratio of ellipticities measured at 222 nm and 216 nm (*D*). *E* was obtained with K57E/E61K. *F* is a control experiment, featuring wild-type 4E-BP1$_{51–67}$ in 40% TFE.

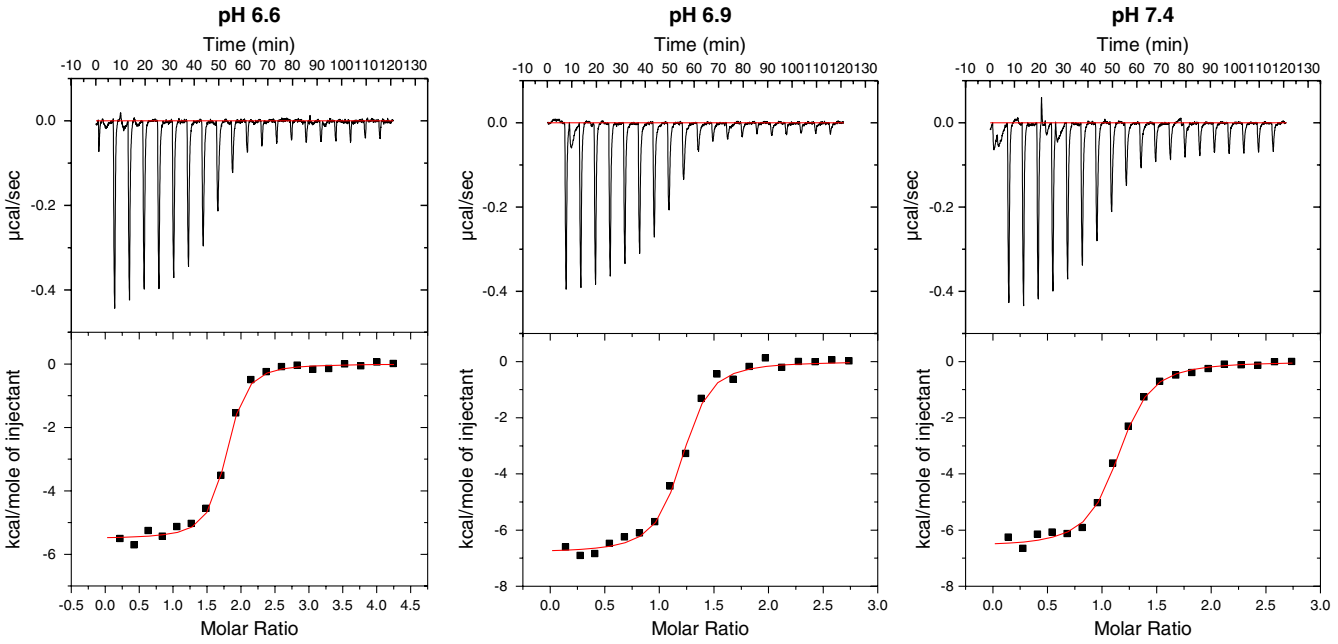

Fig. S2. Isothermal titration calorimetry titrations performed as in Fig. 1 at three different pH values. 4E-BP1$_{51–67}$ phosphorylated on S65 was titrated against wild-type eIF4E.

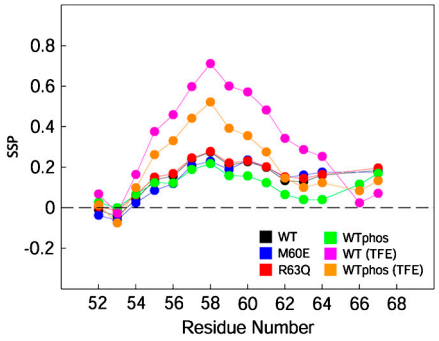

Fig. S3. Secondary structure propensity (SSP) values were calculated for single residues based on Cα, Cβ, and Hα chemical shifts in the ^{13}C, ^{15}N-labeled 4E-BP1$_{51–67}$ peptides according to the procedure outlined in ref. 1. Positive and negative values indicate propensity to form α-helical and β-sheet structures, respectively. The propensity of WT to form α-helix is marginally higher than that of phosphorylated WT (in the absence of TFE; compare black and green). However, the propensity values are significantly different in the presence of TFE (compare magenta and orange), supporting our hypothesis that WT has higher probability to form helix upon interaction with eIF4E.

1. Marsh J, Singh K, Zongchao J, Forman-Kay, JD (2006) Sensitivity of secondary structure propensities to sequence differences between α- and γ- synuclein: Implications for fibrillation. *Protein Sci* 15:2795–2804.

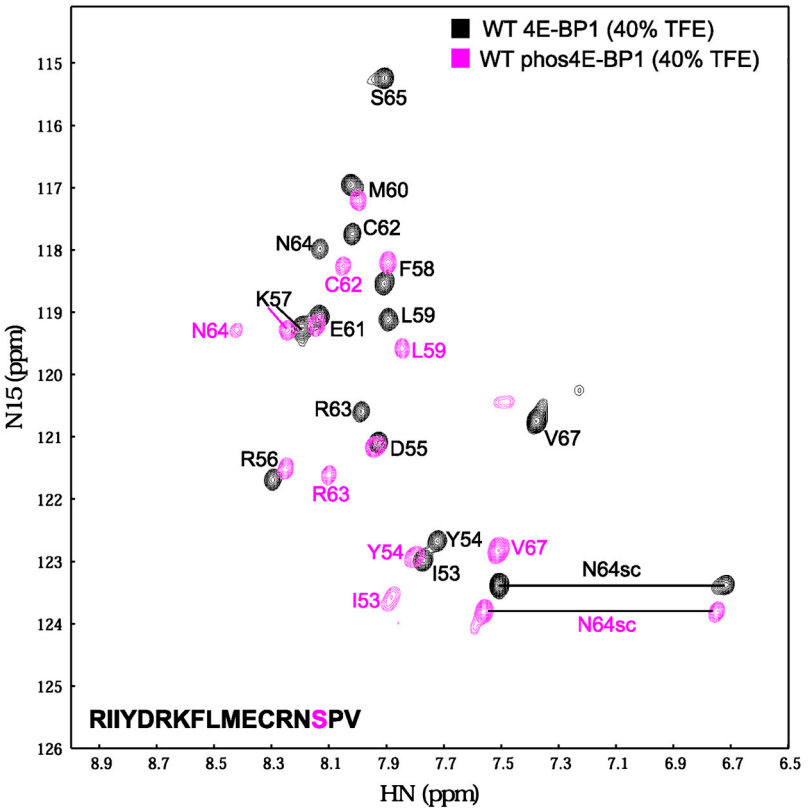

Fig. S4. NMR spectra of WT and phosphorylated 4E-BP1$_{51–67}$ in 40% TFE. Overlaid ^{1}H-^{15}N HSQC spectra of wild-type (black) and S65-phosphorylated (pink) peptides of the 4E-BP1$_{51–67}$ with assignment (see sequence in lower left-hand corner; S65 is highlighted pink).

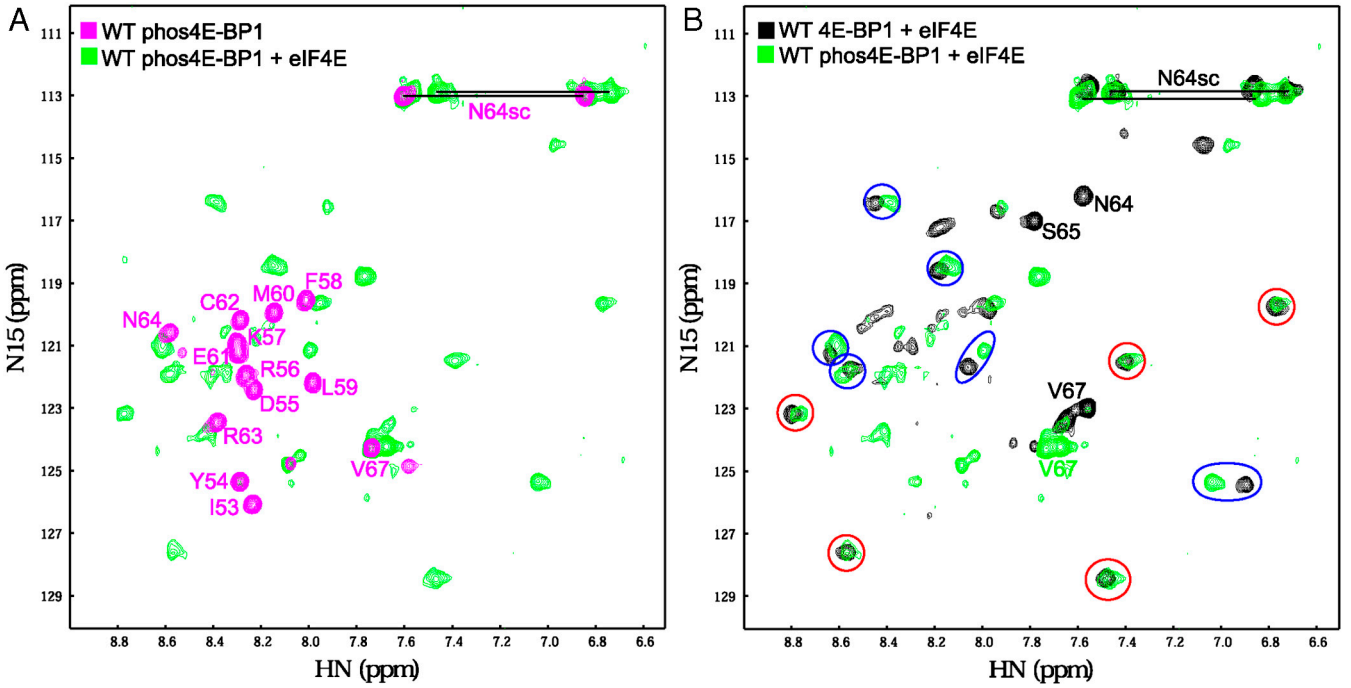

Fig. S5. NMR spectra reveal conformational changes. (*A*) Overlaid ^{1}H-^{15}N HSQC spectra of S65-phosphorylated wild-type 4E-BP1$_{51–67}$ peptide complexed with human eIF4E (green) and of noncomplexed S65-phosphorylated wild-type 4E-BP1$_{51–67}$ peptide (pink). (*B*) Overlaid ^{1}H-^{15}N HSQC spectra of wild-type 4E-BP1$_{51–67}$ peptide complexed with human eIF4E (black) and of S65-phosphorylated wild-type 4E-BP1$_{51–67}$ peptide complexed with human eIF4E (green). Circles identify those residues with minimal shift perturbation (red) and those with significant changes (blue).

Table S1. $J_{HN\text{-}H\alpha}$ values calculated using the 3JHNHα coupling constant (HNHA) experiment for WT, M60E, R63Q mutants and phosphorylated WT 4E-BP1$_{51–67}$

Residue	WT	WT (40% TFE)	M60E	R63Q	WTphos	Wtphos (40% TFE)
I52	—		—	—	8.4	—
I53	9.1	8.0	8.9	9.1	8.9	9.1
Y54	7.9	7.5	8.0	8.3	8.3	8.2
D55	7.4	7.0	7.2	7.5	7.9	7.2
R56	**5.7**	**4.5**	**5.8**	**5.9**	**6.2**	**4.3**
K57	**6.2**	**5.0**	**5.9**	**6.5**	**6.1**	**5.2**
F58	**7.0**	**5.1**	**6.7**	**7.2**	**7.6**	**5.7**
L59	**6.7**	**5.2**	**6.6**	—	**6.6**	**6.3**
M60	**6.9**	**6.0**	**6.3 (E)**	**7.1**	**7.3**	**6.6**
E61	**6.4**	**6.3**	**5.9**	**6.7**	**5.9**	**6.2**
C62	7.7	6.4	7.2	7.6	8.8	7.3
R63	7.5	6.7	7.2	7.4 (Q)	8.6	7.5
N64	8.4	8.0	7.7	8.0	8.5	7.9
S65	7.0	6.9	6.9	7.2	—	—
P66	—	—	—	—	—	—
V67	9.1	9.2	9.1	9.2	9.0	8.9

Residues that form α-helix upon interacting with eIF4E are shown in bold.